SCIENCE CHINA
Information Sciences

• RESEARCH PAPER •
Special Focus on B5G Wireless Communication Networks

August 2019, Vol. 62 080304:1–080304:12
https://doi.org/10.1007/s11432-019-9928-5

Optimal power allocation for secure directional modulation networks with a full-duplex UAV user

Zaoyu LU[1], Linlin SUN[1], Shuo ZHANG[2], Xiaobo ZHOU[1], Jinyong LIN[2], Wenlong CAI[2], Jin WANG[1], Jinhui LU[1] & Feng SHU[1*]

[1]*School of Electronic and Optical Engineering, Nanjing University of Science and Technology, Nanjing* 210094*, China;*
[2]*Beijing Aerospace Automatic Control Institute, Beijing* 100854*, China*

Received 5 April 2019/Revised 11 June 2019/Accepted 28 June 2019/Published online 12 July 2019

Abstract This paper makes an investigation of a secure unmanned aerial vehicle (UAV)-aided communication network based on directional modulation (DM). In this network, ground base station (GBS) acts as a control center to transmit confidential message and artificial noise (AN). The UAV user, moving along a linear flight trajectory, is intended to receive the useful information from GBS. At the same time, it also sends AN signals to further interference eavesdropper's channel. Aiming at maximizing secrecy rate during the UAV flight process, a joint optimization problem is formulated with respect to power allocation (PA) factors, beamforming vector and AN projection matrices. For simplicity, maximum rate transmission, null-space projection and the leakage-based method are applied to form the transmit beamforming vector, AN projection matrix at GBS, and AN projection vector at UAV user, respectively. Following this, the optimization problem reduces to a bivariate optimization programme with two PA factors. An alternating iterative algorithm (AIA) is proposed to optimize the two PA factors. Simulation results demonstrate that, compared to the half-duplex (HD) mode, the proposed strategy for full-duplex (FD) mode achieves a higher secrecy rate (SR) and outperforms the FD mode with fixed PA strategy.

Keywords UAV, directional modulation, secrecy rate, artificial noise, full-duplex, power allocation

Citation Lu Z Y, Sun L L, Zhang S, et al. Optimal power allocation for secure directional modulation networks with a full-duplex UAV user. Sci China Inf Sci, 2019, 62(8): 080304, https://doi.org/10.1007/s11432-019-9928-5

1 Introduction

With diverse potential applications, unmanned aerial vehicles (UAVs)-aided wireless communications have a promising prospect in the coming future [1–4]. UAV has a variety of advantages, such as high mobility, flexible deployment, controllable trajectory and low cost [5–7]. The problems surrounding the UAV-aided networks mainly focus on trajectory optimization, user scheduling, resource allocation, energy harvesting, etc [7–10]. Besides, due to the broadcast characteristic of wireless signals, UAV-aided wireless communications are vulnerable to be hostilely attacked. Consequently, secure wireless transmission in UAV wireless networks is a very challenging issue at present and in the further [11–14]. A cooperative jamming approach in [11] was proposed to secure the UAV communication through utilizing the neighbor UAVs as jammers to defend against the eavesdropper. For the purpose of maximizing the minimum average secrecy rate (SR), the authors in [12] leveraged the alternating iterative algorithm (AIA) and successive convex approximation technique to jointly optimize the trajectories and transmit powers of UAV base station/jammers. The authors of [13] investigated a UAV-enabled secure communication

* Corresponding author (email: shufeng0101@163.com)

system that the UAV trajectories and user scheduling are jointly adjusted to maximize the minimum worst-case SR among the users within each period. In [14], the authors optimized the power allocation (PA) strategy by combining the transmission outage probability and secrecy outage probability as a new performance metric.

Directional modulation (DM), as a key physical layer security (PLS) technology in wireless communication, has attracted a lot of attentions from both academia and industry [15–17]. To further protect the security of UAV communication networks, DM technology has been increasingly applied to UAV network due to the line-of-sight (LoS) aerial-ground link [1, 18, 19]. Artificial noise (AN) is usually utilized to disturb the potential eavesdroppers to improve the PLS in DM networks [20, 21]. The authors in [22] projected the orthogonal AN onto the null-space of the steering vector along the intended direction to enhance the PLS. For the multicast scenarios, both the useful precoding vector and the AN projection matrix can be designed according to the leakage-based criterion [23]. In [24], the authors maximized the SR by the alternating iterative PA strategy, which achieves a significant SR gain in the case of small-scale antenna array. In DM systems, the direction of arrival (DOA) needs to be estimated in advance for the DM synthesis. Two phase alignment methods were proposed to estimate DOA based on the parametric method in [25]. In [26], the authors presented a robust beamforming scheme of combining main-lobe-integration and leakage to further improve the security in DM systems in the presence of direction angle measurement errors. A secure precise wireless transmission with low-complexity structure by random subcarrier selection (RSCS) was proposed in [27].

To improve the spectral efficiency of next-generation wireless networks, full-duplex (FD) transmission has attracted fast-growing attentions [28–32]. In [28], a cooperative FD jammer was introduced to generate the precoded AN for guaranteeing the security of legitimate transmissions without knowing the eavesdropper's channel state information (CSI). In [32], a robust AN-aided amplify-and-forward scheme was proposed to maximize the worst-case sum SR of the eavesdropper without knowing CSI. The authors of [30] designed a FD jamming relay network, in which the relay node transmits jamming signals to interfere the eavesdropper while receives the data from the source at the same time. FD transceivers were also adopted to enhance wireless PLS for multi-hop relaying systems in [29]. When the relays received information signals from the previous adjacent node, they simultaneously transmitted AN signals to the eavesdropper.

Motivated by the above studies, in this paper, we investigate a PA strategy in UAV-aided communication networks where UAV user operates in FD mode. With the purpose of maximizing SR (Max-SR), we formulate a joint optimization problem to design the beamforming vector, AN projection matrix, and PA factors. This problem is very hard to tackle due to the complicated objective function and the coupled variables. For simplicity, maximum ratio transmission (MRT) is applied to form the transmit beamforming vector, the AN projection matrix for Alice is constructed by the null-space projection (NSP) criterion, and the AN projection vector for Bob is designed by the leakage-based method. As such, the optimization problem reduces to a bivariate optimization programme with two PA factors. Using the given PA factor of the ground base station transmitter, we can design the optimal PA factor of legitimate UAV user. Accordingly, with the given PA factor of UAV transmitter, we can derive the optimal PA factor of ground base station. Subsequently, an AIA between two PA factors is proposed to further improve the SR performance. This algorithm is repeated until the terminal condition is satisfied. Simulation results also verify that the SR performance of the proposed strategy achieves a substantial gain over HD mode with fixed PA strategy.

The remainder of the paper is organized as follows. System model is described in Section 2. Section 3 gives the beamforming vector and AN projection vector, and an AIA for PA strategy is proposed to further improve SR performance. Simulation results are shown in Section 4. Finally, Section 5 concludes this paper.

Notations. Throughout the paper, matrices, vectors, and scalars are denoted by letters of bold upper case, bold lower case, and lower case, respectively. Signs $(\cdot)^{\mathrm{T}}$, $(\cdot)^{\mathrm{H}}$, $|\cdot|$ and $\|\cdot\|$ represent transpose, conjugate transpose, modulus and norm, respectively. $\mathbf{I}_N$ denotes the $N \times N$ identity matrix.

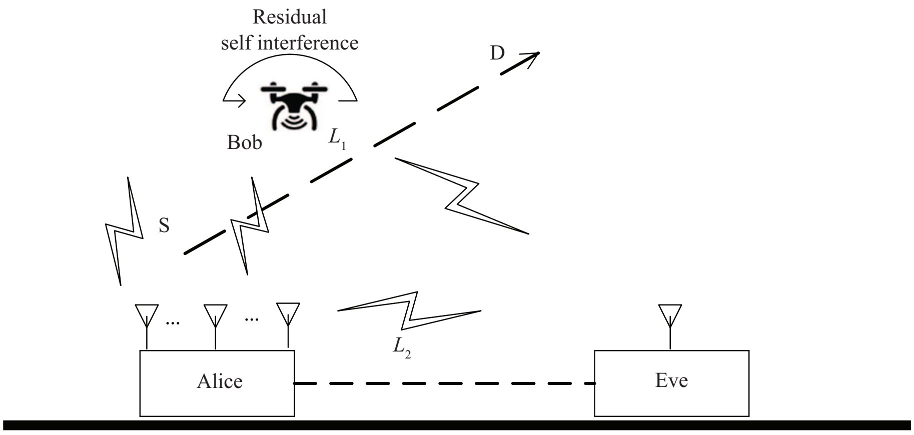

Figure 1 System model with FD UAV receiver.

2 System model

A UAV-enabled wireless communications system is depicted in Figure 1. It consists of an N-antennas base station (Alice), a legitimate N_b-antennas UAV user (Bob) and a potentially illegal single-antenna receiver (Eve). Assuming that Bob flies along an L_1-meters-long direct path from S to D. Bob works in FD mode, that is, it transmits signals with N antennas while simultaneously receives messages with the remaining $N_b - N$ antennas. As mentioned in [18, 19], the link from ground station to the UAV user can be viewed as a line-of-sight (LoS) channel, we set $N_b - N = 1$.

Due to the broadcasting characteristic of wireless communications, the confidential messages conveyed from Alice to Bob are vulnerable to be eavesdropped by Eve. Two ways are used to solve this problem. For the source node, AN signals are superimposed on the confidential messages to prevent the useful information being wiretapped. From the perspective of the destination node, Bob helps itself by operating in FD mode and transmitting AN signals to worsen the quality of Alice-to-Eve link. The transmit baseband signal from Alice is expressed as

$$\boldsymbol{s} = \sqrt{\beta_1 P_a}\boldsymbol{v}_b x + \sqrt{(1-\beta_1)P_a}\boldsymbol{P}_{\rm AN}\boldsymbol{z}, \tag{1}$$

where P_a is the total transmit power at Alice, β_1 and $(1-\beta_1)$ stand for the PA factors for confidential message and AN, respectively. x is the confidential message satisfying $\mathbb{E}\left\{x^{\rm H}x\right\} = 1$, and $\boldsymbol{z} \in \mathbb{C}^{N\times 1}$ means the AN vector obeying complex Gaussian distribution, i.e., $\boldsymbol{z} \sim \mathcal{CN}(\boldsymbol{0}, \mathbf{I}_N)$. $\boldsymbol{v}_b \in \mathbb{C}^{N\times 1}$ denotes the transmit beamforming vector for controlling the confidential messages to the desired direction, and $\boldsymbol{P}_{\rm AN} \in \mathbb{C}^{N\times N}$ is the projection matrix leading AN to the undesired direction, $\boldsymbol{v}_b^{\rm H}\boldsymbol{v}_b = 1$ and ${\rm Tr}\{\boldsymbol{P}_{\rm AN}\boldsymbol{P}_{\rm AN}^{\rm H}\} = 1$.

The corresponding received signal at Bob can be written as

$$y_b = \sqrt{g_{ab}\beta_1 P_a}\boldsymbol{h}_{sd}^{\rm H}\boldsymbol{v}_b x + \sqrt{g_{ab}(1-\beta_1)P_a}\boldsymbol{h}_{sd}^{\rm H}\boldsymbol{P}_{\rm AN}\boldsymbol{z} + \sqrt{\beta_2 P_b \rho}\boldsymbol{h}_{dd}^{\rm H}\boldsymbol{q}_{\rm AN} z + n_b, \tag{2}$$

where $z \sim \mathcal{CN}(0,1)$ denotes the scalar AN, and the complex additive white Gaussian noise (AWGN) at Bob is denoted by $n_b \sim \mathcal{CN}(0, \sigma_b^2)$. P_b represents the total transmit power at Bob. It is noted that if AN signal z with sent at full power, it will generate a strong self-interference. Hence, β_2 is introduced to regulate the transmit power of AN signal. $g_{ab} = \frac{\alpha}{d_{ab}^c}$ represents the path loss from Alice to Bob. Here, d_{ab} is the distance between Alice and Bob, c denotes the path loss exponent and α means the path loss at reference distance d_0. $\boldsymbol{h}_{sd} \in \mathbb{C}^{N\times 1}$ represents the steering vector from Alice to Bob, and $\boldsymbol{h}_{dd} \in \mathbb{C}^{N\times 1}$ is the loop-channel between the receiving and the transmitting antennas of Bob. $\boldsymbol{q}_{\rm AN} \in \mathbb{C}^{N\times 1}$ stands for the projection matrix leading AN signal sent from Bob to the undesired direction with $\boldsymbol{q}_{\rm AN}^{\rm H}\boldsymbol{q}_{\rm AN} = 1$. $\rho \in [0,1]$ is introduced to represent the proportion of residual self-interference after antenna and radio-frequency cancellation.

In the same manner, the receive signal at Eve is given by

$$y_e = \sqrt{g_{ae}\beta_1 P_a}\boldsymbol{h}_{se}^{\rm H}\boldsymbol{v}_b x + \sqrt{g_{ae}(1-\beta_1)P_a}\boldsymbol{h}_{se}^{\rm H}\boldsymbol{P}_{\rm AN}\boldsymbol{z} + \sqrt{g_{be}\beta_2 P_b}\boldsymbol{h}_{de}^{\rm H}\boldsymbol{q}_{\rm AN} z + n_e, \tag{3}$$

where $g_{ae} = \frac{\alpha}{d_{ae}^c}$ denotes the path loss from Alice to Eve, and d_{ae} is the distance between Alice and Eve. $g_{be} = \frac{\alpha}{d_{be}^c}$ represents the path loss from Bob to Eve, and d_{be} means the distance between Alice and Eve. $\boldsymbol{h}_{se} \in \mathbb{C}^{N\times 1}$ denotes the steering vector from Alice to Eve, and $\boldsymbol{h}_{de} \in \mathbb{C}^{N\times 1}$ denotes the steering vector from Bob to Eve. $n_e \sim \mathcal{CN}(0, \sigma_e^2)$ is the complex AWGN at Eve.

For DM systems, the steering vectors in (2) and (3) have the following form:

$$\boldsymbol{h}(\theta) = \frac{1}{\sqrt{N}}\left[\mathrm{e}^{\mathrm{j}2\pi\Psi_\theta(1)}, \dots, \mathrm{e}^{\mathrm{j}2\pi\Psi_\theta(n)}, \dots, \mathrm{e}^{\mathrm{j}2\pi\Psi_\theta(N)}\right]^{\mathrm{T}}, \tag{4}$$

and the phase function $\Psi_\theta(n)$ is defined by

$$\Psi_\theta(n) \triangleq -\frac{(n-(N+1)/2)d\cos\theta}{\lambda}, \quad n = 1, 2, \dots, N, \tag{5}$$

where n indexes the antenna, d represents the antenna spacing, θ denotes the directional angle, and λ means the carrier wavelength of transmit signal.

As per (2) and (3), the achievable rates from Alice to Bob and Eve can be expressed as

$$R_b = \log_2\left(1 + \frac{g_{ab}P_a\beta_1\boldsymbol{h}_{sd}^{\mathrm{H}}\tilde{\boldsymbol{V}}\boldsymbol{h}_{sd}}{g_{ab}(1-\beta_1)P_a\boldsymbol{h}_{sd}^{\mathrm{H}}\tilde{\boldsymbol{P}}\boldsymbol{h}_{sd} + \beta_2 P_b\rho\boldsymbol{h}_{dd}^{\mathrm{H}}\tilde{\boldsymbol{Q}}\boldsymbol{h}_{dd} + \sigma_b^2}\right), \tag{6}$$

and

$$R_e = \log_2\left(1 + \frac{g_{ae}P_a\beta_1\boldsymbol{h}_{se}^{\mathrm{H}}\tilde{\boldsymbol{V}}\boldsymbol{h}_{se}}{g_{ae}(1-\beta_1)P_a\boldsymbol{h}_{se}^{\mathrm{H}}\tilde{\boldsymbol{P}}\boldsymbol{h}_{se} + g_{be}\beta_2 P_b\boldsymbol{h}_{de}^{\mathrm{H}}\tilde{\boldsymbol{Q}}\boldsymbol{h}_{de} + \sigma_e^2}\right), \tag{7}$$

where $\tilde{\boldsymbol{V}} = \boldsymbol{v}_b\boldsymbol{v}_b^{\mathrm{H}}$, $\tilde{\boldsymbol{P}} = \boldsymbol{P}_{\mathrm{AN}}\boldsymbol{P}_{\mathrm{AN}}^{\mathrm{H}}$ and $\tilde{\boldsymbol{Q}} = \boldsymbol{q}_{\mathrm{AN}}\boldsymbol{q}_{\mathrm{AN}}^{\mathrm{H}}$.

As such, the achievable SR will become

$$R_s = \max\{0, R_b - R_e\}. \tag{8}$$

To maximize the above R_s, we need to solve the following optimization problem, that is

$$\begin{aligned}
(\mathrm{P1}): \quad & \max_{\beta_1,\beta_2,\boldsymbol{v}_b,\boldsymbol{P}_{\mathrm{AN}},\boldsymbol{q}_{\mathrm{AN}}} \quad R_s && \text{(9a)}\\
& \text{s.t.} \quad 0 \leqslant \beta_1 \leqslant 1, && \text{(9b)}\\
& \quad\quad\; 0 \leqslant \beta_2 \leqslant 1, && \text{(9c)}\\
& \quad\quad\; \boldsymbol{v}_b^{\mathrm{H}}\boldsymbol{v}_b = 1, && \text{(9d)}\\
& \quad\quad\; \mathrm{Tr}\{\boldsymbol{P}_{\mathrm{AN}}^{\mathrm{H}}\boldsymbol{P}_{\mathrm{AN}}\} = 1, && \text{(9e)}\\
& \quad\quad\; \boldsymbol{q}_{\mathrm{AN}}^{\mathrm{H}}\boldsymbol{q}_{\mathrm{AN}} = 1, && \text{(9f)}
\end{aligned}$$

where (9b) and (9c) are the PA constraint of the transmitter and the UAV, respectively, while (9d), (9e) and (9f) are the power constraint of the confidential information beamforming vector $\boldsymbol{v}_b$, the AN project matrix $\boldsymbol{P}_{\mathrm{AN}}$ and the AN beamforming vector $\boldsymbol{q}_{\mathrm{AN}}$, respectively. It is noted that problem (P1) is non-convex due to the non-convex objective function and non-convex constraint set. Furthermore, the optimization variables in (P1) are coupled. As such, it is difficult to address problem (P1) directly. Fortunately, if the beamforming vector $\boldsymbol{v}_b$, $\boldsymbol{P}_{\mathrm{AN}}$ and $\boldsymbol{q}_{\mathrm{AN}}$ are designed or fixed in advance, the joint optimization will reduce to the following bivariate PA problem

$$\begin{aligned}
(\text{P1-1}): \quad & \max_{\beta_1,\beta_2} \quad R_s \\
& \text{s.t.} \quad 0 \leqslant \beta_1 \leqslant 1, \\
& \quad\quad\; 0 \leqslant \beta_2 \leqslant 1.
\end{aligned} \tag{10}$$

For simplicity, we rewrite $R_b - R_e$ as

$$R_b - R_e = \log_2\left(1 + \frac{A\beta_1}{(1-\beta_1)B + \beta_2 C + \sigma_b^2}\right) - \log_2\left(1 + \frac{D\beta_1}{(1-\beta_1)E + \beta_2 F + \sigma_e^2}\right), \tag{11}$$

where

$$\begin{aligned} A &= g_{ab}P_a\boldsymbol{h}_{sd}^{\rm H}\tilde{\boldsymbol{V}}\boldsymbol{h}_{sd},\\ B &= g_{ab}P_a\boldsymbol{h}_{sd}^{\rm H}\tilde{\boldsymbol{P}}\boldsymbol{h}_{sd},\\ C &= P_b\rho\boldsymbol{h}_{dd}^{\rm H}\tilde{\boldsymbol{Q}}\boldsymbol{h}_{dd},\\ D &= g_{ae}P_a\boldsymbol{h}_{se}^{\rm H}\tilde{\boldsymbol{V}}\boldsymbol{h}_{se},\\ E &= g_{ae}P_a\boldsymbol{h}_{se}^{\rm H}\tilde{\boldsymbol{P}}\boldsymbol{h}_{se},\\ F &= g_{be}P_b\boldsymbol{h}_{de}^{\rm H}\tilde{\boldsymbol{Q}}\boldsymbol{h}_{de}. \end{aligned} \tag{12}$$

Let $R_b - R_e = F(\beta_1, \beta_2)$, optimization problem (10) can be further reduced to

$$\begin{aligned} (\text{P1-2}):\quad & \max_{\beta_1,\beta_2} \quad \max\{0, F(\beta_1,\beta_2)\}\\ & \text{s.t.} \quad 0 \leqslant \beta_1 \leqslant 1,\\ & \qquad\;\; 0 \leqslant \beta_2 \leqslant 1. \end{aligned} \tag{13}$$

For the above objective function, the following equation holds:

$$\max_{\beta_1,\beta_2} \ \max\{0, F(\beta_1,\beta_2)\} = \max\{0, \max_{\beta_1,\beta_2} \ F(\beta_1,\beta_2)\}. \tag{14}$$

Since $F(\beta_1, \beta_2) = 0$ is feasible at $\beta_1 = 0$, we have

$$\max_{\beta_1,\beta_2} F(\beta_1,\beta_2) \geqslant 0. \tag{15}$$

Herein, the optimization problem (13) reduces to

$$\begin{aligned} (\text{P1-3}):\quad & \max_{\beta_1,\beta_2} \quad F(\beta_1,\beta_2)\\ & \text{s.t.} \quad 0 \leqslant \beta_1 \leqslant 1,\\ & \qquad\;\; 0 \leqslant \beta_2 \leqslant 1. \end{aligned} \tag{16}$$

In other words, the optimization problem (10) is equivalent to

$$\begin{aligned} (\text{PA1}):\quad & \max_{\beta_1,\beta_2} \quad F(\beta_1,\beta_2) = \log_2\frac{-A_2\beta_1^2 + B_1\beta_2^2 + C_2\beta_1\beta_2 + D_2\beta_1 + E_1\beta_2 + F_1}{-A_1\beta_1^2 + B_1\beta_2^2 + C_1\beta_1\beta_2 + D_1\beta_1 + E_1\beta_2 + F_1}\\ & \text{s.t.} \quad 0 \leqslant \beta_1 \leqslant 1,\\ & \qquad\;\; 0 \leqslant \beta_2 \leqslant 1. \end{aligned} \tag{17}$$

where

$$\begin{aligned} & A_1 = B(D-E), \quad B_1 = CF, \quad C_1 = C(D-E) - BF,\\ & D_1 = (D-E)(B+\sigma_b^2) - B(E+\sigma_b^2),\\ & E_1 = C(E+\sigma_e^2) + F(B+\sigma_b^2),\\ & F_1 = (B+\sigma_b^2)(E+\sigma_e^2),\\ & A_2 = E(A-B),\\ & C_2 = F(A-B) - CE,\\ & D_2 = (A-B)(E+\sigma_e^2) - E(B+\sigma_b^2). \end{aligned} \tag{18}$$

Observing (17), the expression of function $F(\beta_1, \beta_2)$ indicates that R_s is continuous and differentiable with respect to β_1, β_2 in the interval $[0, 1]$. Hence, the promising optimal β_1 and β_2 must be either endpoints or stationary points. As such, we need to find out all the stationary points by vanishing the first-order derivative of $F(\beta_1, \beta_2)$ with respect to β_1 and β_2. On this basis, the optimal β_1, β_2 will be selected by comparing the values of $F(\beta_1, \beta_2)$ among the set of all candidate points to the critical numbers.

3 Proposed PA strategy of max-SR

In this section, we employ NSP scheme to guarantee that the legitimate UAV receiver will not be affected by the AN signal, while at the same time the potentially illegal eavesdropper will be seriously distorted. Besides, from the aspect of Bob, the AN signal transmitted by Bob will interfere the Alice-to-Eve link and minimize AN signal leakage to itself. Then the PA factors are iteratively solved.

3.1 Design $\boldsymbol{v_b}$, $\boldsymbol{P}_{\mathbf{AN}}$ and $\boldsymbol{q}_{\mathbf{AN}}$

First, MRT is applied to form the transmit beamforming vector at Alice,

$$\boldsymbol{v}_b = \boldsymbol{h}_{sd}. \tag{19}$$

In order to make AN signal emitted by Alice free of any interference to Bob, $\boldsymbol{P}_{\rm AN}$ is designed to project $\boldsymbol{z}$ into the null space of $\boldsymbol{h}_{sd}^{\rm H}$. Therefore, the projection matrix $\boldsymbol{P}_{\rm AN}$ is given by

$$\boldsymbol{P}_{\rm AN} = \mathbf{I}_N - \boldsymbol{h}_{sd}\boldsymbol{h}_{sd}^{\rm H}. \tag{20}$$

To further interfere with Eve, Bob will also transmit AN signal, which generates a strong self-interference. Motivated by this, we design beamforming vector $\boldsymbol{q}_{\rm AN}$ to minimize the AN signal leakage to Bob, called maximizing AN-to-leakage-and-noise ratio (ANLNR),

$$\begin{aligned} ({\rm P2}):\ \ & \max_{\boldsymbol{q}_{\rm AN}} \quad {\rm ANLNR}(\boldsymbol{q}_{\rm AN}) \\ & \ {\rm s.t.} \quad \boldsymbol{q}_{\rm AN}^{\rm H}\boldsymbol{q}_{\rm AN} = 1, \end{aligned} \tag{21}$$

where

$$\mathrm{ANLNR}(\boldsymbol{q}_{\rm AN}) = \frac{\beta_2 P_b \boldsymbol{q}_{\rm AN}^{\rm H}\boldsymbol{h}_{de}\boldsymbol{h}_{de}^{\rm H}\boldsymbol{q}_{\rm AN}}{\boldsymbol{q}_{\rm AN}^{\rm H}(\beta_2 P_b \boldsymbol{h}_{dd}\boldsymbol{h}_{dd}^{\rm H} + \sigma_e^2\mathbf{I}_N)\boldsymbol{q}_{\rm AN}}. \tag{22}$$

Using the generalized Rayleigh-Ritz ratio theorem in [33], the optimal $\boldsymbol{q}_{\rm AN}$ can be obtained from the eigenvector corresponding to the largest eigen-value of the matrix:

$$[\beta_2 P_b \boldsymbol{h}_{dd}\boldsymbol{h}_{dd}^{\rm H} + \sigma_e^2\mathbf{I}_N]^{-1}\boldsymbol{h}_{de}\boldsymbol{h}_{de}^{\rm H}. \tag{23}$$

Notice that the above matrix is rank-one, we can obtain the closed-form solution to (21) as

$$\boldsymbol{q}_{\rm AN} = \frac{[\beta_2 \boldsymbol{h}_{dd}\boldsymbol{h}_{dd}^{\rm H} P_b + \sigma_e^2\mathbf{I}_N]^{-1}\boldsymbol{h}_{de}}{\|[\beta_2 \boldsymbol{h}_{dd}\boldsymbol{h}_{dd}^{\rm H} P_b + \sigma_e^2\mathbf{I}_N]^{-1}\boldsymbol{h}_{de}\|_2}. \tag{24}$$

On this basis, we will detail the PA scheme to solve β_1 for fixed β_2 in what follows.

3.2 Optimize $\boldsymbol{\beta_1}$ for fixed $\boldsymbol{\beta_2}$

Given a fixed β_2, the stationary points with respect to β_1 should satisfy the following equation:

$$\begin{aligned} \frac{\partial F(\beta_1, \text{fixed } \beta_2)}{\partial \beta_1} &= \frac{(A_1B_3 - A_2D_3)\beta_1^2 + 2(A_1C_3 - A_2C_3)\beta_1 + B_3C_3 - C_3D_3}{(-A_1\beta_1^2 + D_3\beta_1 + C_3)^2} \\ &= 0, \end{aligned} \tag{25}$$

where

$$\begin{aligned} B_3 &= D_2 + C_2\beta_2, \\ C_3 &= (E_1 + B_1\beta_2)\beta_2 + F_1, \\ D_3 &= D_1 + C_1\beta_2, \end{aligned} \tag{26}$$

which yields

$$\beta_{1,1} = \frac{-(A_1C_3 - A_2C_3) + \sqrt{\Delta_1}}{A_1B_3 - A_2D_3}, \tag{27}$$

$$\beta_{1,2} = \frac{-(A_1C_3 - A_2C_3) - \sqrt{\Delta_1}}{A_1B_3 - A_2D_3}, \tag{28}$$

where

$$\Delta_1 = (A_1C_3 - A_2C_3)^2 - (A_1B_3 - A_2D_3)(B_3C_3 - C_3D_3). \tag{29}$$

Considering $\beta_1 \in [0, 1]$, we obtain the candidate set for the critical numbers of function $F(\beta_1, \text{fixed } \beta_2)$ as

$$S_1(\text{fixed } \beta_2) = \{0, \beta_{1,1}, \beta_{1,2}, 1\}. \tag{30}$$

In the following, we need to decide which β_1 is the optimal solution to maximize the function $F(\beta_1, \text{fixed } \beta_2)$ in the four candidate points. Obviously, $\beta_1 = 0$ means that there is no confidential messages transmitted to Bob. Thus, $\beta_1 = 0$ should be removed from the above candidate set. Now we only need to discuss the remaining three candidate points $F(\beta_{1,1}, \text{fixed } \beta_2)$, $F(\beta_{1,2}, \text{fixed } \beta_2)$ and $F(1, \text{fixed } \beta_2)$.

Below, let us discuss this issue in different cases of Δ_1. The first case is $\Delta_1 < 0$, then the two real roots $\beta_{1,1}$ and $\beta_{1,2}$ will not exist. On this basis, we need to check the following three cases.

Case 1. $A_1B_3 - A_2D_3 > 0$, $F(\beta_1, \text{fixed } \beta_2)$ is a monotonously increasing function and will achieve its maximum value at $\beta_1 = 1$.

Case 2. $A_1B_3 - A_2D_3 = 0$, the stationary point is $\beta_{1,3} = \frac{C_3D_3 - B_3C_3}{2(A_1C_3 - A_2C_3)}$. We obtain the PA factor β_1 by comparing the value of $F(\beta_{1,3}, \text{fixed } \beta_2)$ and $F(1, \text{fixed } \beta_2)$.

Case 3. $A_1B_3 - A_2D_3 < 0$, $F(\beta_1, \text{fixed } \beta_2)$ is a monotonously decreasing function of β_1. Therefore, the PA factor is $\beta_1 = 0$. This result makes to a contradict with what was discussed above.

The second case is $\Delta_1 \geqslant 0$, we need to judge whether $\beta_{1,1}$ and $\beta_{1,2}$ meet the condition that the PA factor β_1 lies in the interval of (0, 1). Then, compare the values of $F(\beta_1, \text{fixed } \beta_2)$ at the endpoints and corresponding stationary points to get the β_1. There are four different cases.

Case 1. If $\beta_{1,1} \in (0, 1)$, $\beta_{1,2} \in (0, 1)$, then compare the values of $F(\beta_{1,1}, \text{fixed } \beta_2)$, $F(\beta_{1,2}, \text{fixed } \beta_2)$ and $F(1, \text{fixed } \beta_2)$.

Case 2. If $\beta_{1,1} \in (0, 1)$, $\beta_{1,2} \notin (0, 1)$, then compare the values of $F(\beta_{1,1}, \text{fixed } \beta_2)$ and $F(1, \text{fixed } \beta_2)$.

Case 3. If $\beta_{1,1} \notin (0, 1)$, $\beta_{1,2} \in (0, 1)$, then compare the values of $F(\beta_{1,2}, \text{fixed } \beta_2)$ and $F(1, \text{fixed } \beta_2)$.

Case 4. If $\beta_{1,1} \notin (0, 1)$, $\beta_{1,2} \notin (0, 1)$, then the value of $\beta = 1$ will be the solution.

After the above discussion, we can get the transmit PA factor β_1 for Alice.

3.3 Optimize β_2 for fixed β_1

Similarly, the stationary points with respect to β_2 for fixed β_1 can be found out by

$$\frac{\partial F(\text{fixed } \beta_1, \beta_2)}{\partial \beta_2} = \frac{(B_1D_4 - B_1B_4)\beta_2^2 + 2(B_1E_4 - B_1C_4)\beta_2 + B_4E_4 - C_4D_4}{(B_1\beta_2^2 + D_4\beta_2 + E_4)^2} = 0, \tag{31}$$

where

$$\begin{aligned} B_4 &= E_1 + C_2\beta_1, \\ C_4 &= (D_2 - A_2\beta_1)\beta_1 + F_1, \\ D_4 &= E_1 + C_1\beta_1, \\ E_4 &= (D_1 - A_1\beta_1)\beta_1 + F_1, \end{aligned} \tag{32}$$

which yields

$$\beta_{2,1} = \frac{-(B_1E_4 - B_1C_4) + \sqrt{\Delta_2}}{B_1D_4 - B_1B_4}, \tag{33}$$

$$\beta_{2,2} = \frac{-(B_1E_4 - B_1C_4) - \sqrt{\Delta_2}}{B_1D_4 - B_1B_4}, \tag{34}$$

where

$$\Delta_2 = (B_1E_4 - B_1C_4)^2 - (B_1D_4 - B_1B_4)(B_4E_4 - C_4D_4). \tag{35}$$

Now, we obtain the candidate set of β_2 for the critical numbers of function $F(\text{fixed } \beta_1, \beta_2)$ as

$$S_2(\text{fixed } \beta_1) = \{0, \beta_{2,1}, \beta_{2,2}, 1\}. \tag{36}$$

From the aspect of legitimate UAV receiver, $\beta_2 = 0$ means that there is no AN sent from Bob. This case happens when the receive signal at Eve is so weak that Bob has no need to send AN signal to interfere with the eavesdropper. On the contrary, when the AN signal transmitted from Alice is fairly weak, $\beta_2 = 1$ may be suitable for Bob to mostly disturb Eve. Overall, there are four candidate points $F(\text{fixed } \beta_1, 0)$, $F(\text{fixed } \beta_1, \beta_{2,1})$, $F(\text{fixed } \beta_1, \beta_{2,2})$ and $F(\text{fixed } \beta_1, 1)$ that we need to judge.

In the same way with β_1, we discuss $\beta_{2,1}$, and $\beta_{2,2}$ in different cases of Δ_2, the first case is $\Delta_2 < 0$.

Case 1. $B_1D_4 - B_1B_4 > 0$, $F(\text{fixed } \beta_1, \beta_2)$ is a monotonously increasing function. It will achieve the maximum value at $\beta_2 = 1$.

Case 2. $B_1D_4 - B_1B_4 = 0$, the stationary point is $\beta_{2,3} = \frac{C_4D_4 - B_4E_4}{2(B_1E_4 - B_1C_4)}$. We obtain the PA factor β_2 by comparing the value of $F(\text{fixed } \beta_1, 0)$, $F(\text{fixed } \beta_1, \beta_{2,3})$ and $F(\text{fixed } \beta_1, 1)$.

Case 3. $B_1D_4 - B_1B_4 < 0$, $F(\text{fixed } \beta_1, \beta_2)$ is a monotonously decreasing function. Therefore, the PA factor is set as $\beta_2 = 0$.

For the second case $\Delta_2 \geqslant 0$, we should judge whether the $\beta_{2,1}$ and $\beta_{2,2}$ meets the condition that the PA factor β_2 lies in the interval of (0, 1). Then, compare the values of $F(\text{fixed } \beta_1, \beta_2)$ at the endpoints and corresponding stationary points to get the β_2. There are also four different cases.

Case 1. If $\beta_{2,1} \in (0, 1)$, $\beta_{2,2} \in (0, 1)$, then compare the values of $F(\text{fixed } \beta_1, 0)$, $F(\text{fixed } \beta_1, \beta_{2,1})$, $F(\text{fixed } \beta_1, \beta_{2,2})$ and $F(\text{fixed } \beta_1, 1)$.

Case 2. If $\beta_{2,1} \in (0, 1)$, $\beta_{2,2} \notin (0, 1)$, then compare the values of $F(\text{fixed } \beta_1, 0)$, $F(\text{fixed } \beta_1, \beta_{2,1})$ and $F(\text{fixed } \beta_1, 1)$.

Case 3. If $\beta_{2,1} \notin (0, 1)$, $\beta_{2,2} \in (0, 1)$, then compare the values of $F(\text{fixed } \beta_1, 0)$, $F(\text{fixed } \beta_1, \beta_{2,2})$ and $F(\text{fixed } \beta_1, 1)$.

Case 4. If $\beta_{2,1} \notin (0, 1)$, $\beta_{2,2} \notin (0, 1)$, then compare the value of $F(\text{fixed } \beta_1, 0)$ and $F(\text{fixed } \beta_1, 1)$.

To this end, we can obtain the transmit PA factor β_2 for the UAV user.

3.4 Proposed AIA

After the above discussion, we can get the optimal PA factor $\beta_1(\beta_2)$ when $\beta_2(\beta_1)$ is given. Now, we propose an AIA from the aspect of further improving SR performance. This AIA is established between β_1^i and β_2^i with an initial value of β_2^0, where superscript i indicates the ith iteration. Then, the feasible PA factor β_1^0 can be obtained from (25) and finally selected from three candidates via aforementioned two scenarios. Subsequently, with the value of β_1^0, we compute the values of β_2^1 based on (31) and select the optimal PA factor from four candidates as aforementioned. This process will be repeated until $|F(\beta_1^i, \beta_2^i) - F(\beta_1^{i-1}, \beta_2^{i-1})|$ is smaller than a preset small value. To make clear, the iterative algorithm is summarized as Algorithm 1.

4 Simulation and discussion

To evaluate the SR performance of the proposed strategy, simulation results are presented in this section. The system parameters are set as: the antenna spacing is $d = \lambda/2$, the path loss exponent $c = 2$, the desired direction is 22°, undesired direction is 30°, the distance between S to D is $L_1 = 400$ m, the distance between Alice and Eve is $L_2 = 200$ m, the UAV speed is $v = 10$ m/s. To ensure the comparison fairness, the transmit power used in HD mode is the summation of the Alice itself and the actual transmit power of Bob.

Algorithm 1 Proposed AIA

Initialization: $i = 0, \beta_2^i = 0.1, R_s^i = 0$.

1. For given β_2^i, solve (25) to obtain the two stationary points (27) and (28);
2. Discuss the aforementioned two scenarios to obtain optimal β_1^i;
3. Solve (31) with the fixed β_1^i, and obtain the two stationary points (33) and (34);
4. Discuss the aforementioned two scenarios to obtain β_2^{i+1};
5. Update $\beta_2^i = \beta_2^{i+1}, i = i + 1$;
6. Compute R_s^i;
7. Until $|F(\beta_1^i, \beta_2^i) - F(\beta_1^{i-1}, \beta_2^{i-1})| \leqslant \epsilon$.

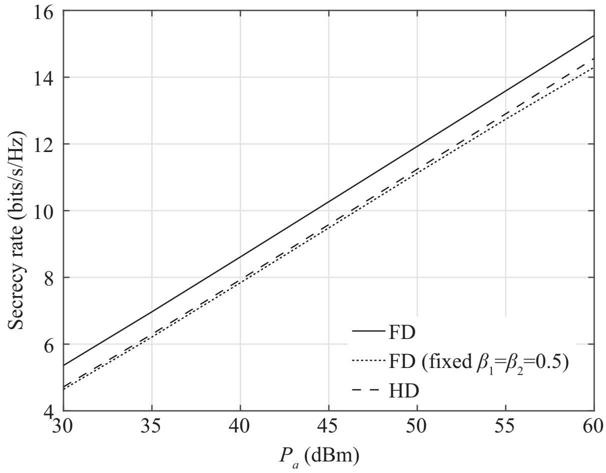

Figure 2 Curves of SR versus P_a for three methods.

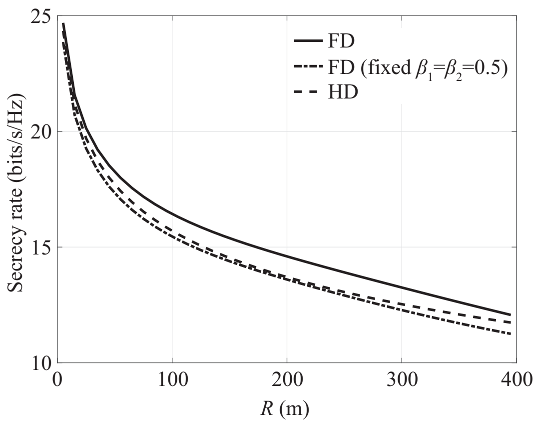

Figure 3 Curves of SR versus R for three methods.

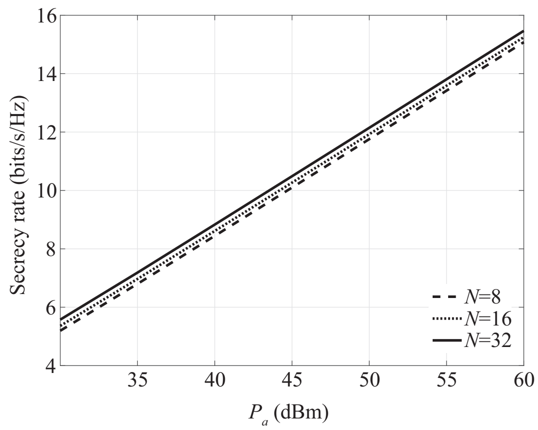

Figure 4 Curves of SR versus P_a for different number of antennas.

Figure 2 plots the curves of SR versus P_a for the proposed PA strategy when the UAV user operates in FD mode and HD mode. For comparison, the FD mode with fixed PA factor is also used as a performance reference. From Figure 2, it is clearly seen that the SR increases gradually with the transmit power P_a no matter Bob operates in FD or HD mode. For any fixed transmit power P_a, it is obvious that the FD mode achieves a substantial SR performance gain over the HD mode and shows a great improvements over the case of fixed PA factor. However, the HD mode achieves a slight SR performance gain over the FD mode with fixed PA factor $\beta_1 = \beta_2 = 0.5$. It reveals that FD mode is not always more reliable than HD mode because of the existence of inevitable self-interference. This also verifies that, for the FD UAV

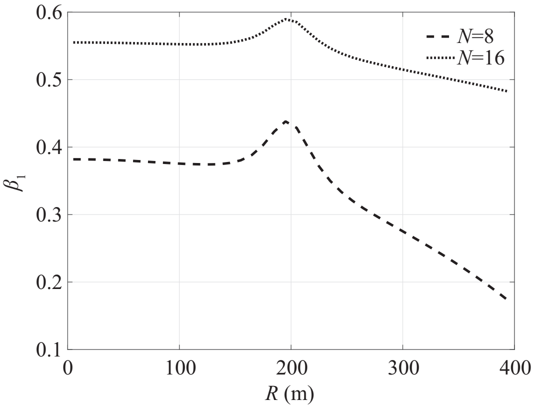

Figure 5 Curves of β_1 versus distance between Alice and Bob for the proposed strategy.

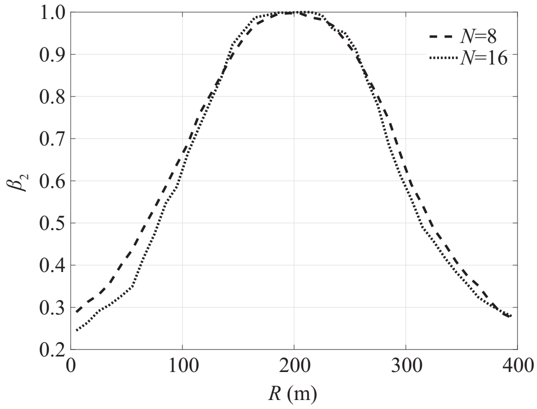

Figure 6 Curves of β_2 versus distance between Alice and Bob for the proposed strategy.

user, our proposed PA strategy is valid to achieve a power balance between the efficient AN signal and redundant self-interference.

Figure 3 shows the curves of SR versus R (the flight distance between Bob and Alice) for the proposed strategy when the UAV user operates in FD mode and HD mode. Also, the FD mode with fixed PA factors is taken into consideration as $\beta_1 = \beta_2 = 0.5$. From this figure, we can observe that the proposed strategy in FD mode shows a substantial improvement over the case of HD mode. And the optimal PA factors generated by the proposed iterative algorithm is superior to the fixed case from the aspect of SR performance.

Figure 4 illustrates the curves of SR versus P_a for different numbers of antennas when the UAV user operates in HD mode with the proposed strategy. It is obvious that when the transmit power is fixed, increasing the number of antennas can increase the SR performance. Therefore, we can add the number of antennas to reduce the transmit power and deploy more antennas to make up for the SR.

Figure 5 shows the curves of β_1 versus the flight distance between Alice and Bob (R) for the proposed strategy. It can be clearly seen that as R is close to the distance between Alice and Eve (L_2), β_1 increases. Particularly, β_1 achieves the maximum value at $R = L_2$. Conversely, when Bob flies farther away from the distance between Alice and Eve ($R > L_2$), β_1 decreases. It reveals that Alice allocates more power to transmit confidential messages when Bob flies near Eve, and more power is used to generate AN signals when Bob flies farther away from Eve to Alice. In addition, we can obviously observe that at a fixed position, β_1 increases as the number of transmit antennas increases. This means that more power is allocated to Alice in order to send confidential messages. This accounts for the reason that deploying more antennas will result in an improvement on SR performance as shown in Figure 4.

Compared with Figure 5, Figure 6 illustrates the curves of β_2 versus the flight distance between Bob and Alice for the proposed strategy. It is seen from this figure that when Bob flies towards Eve ($R < L_2$), it requires more power to transmit AN against the eavesdropper. And when it flies far away from Alice ($R > L_2$), the allocated AN power will reduce. All these curves show us the fact that the eavesdropper becomes sensitive when $|R - L_2|$ approaches zero, in which case, Alice and Bob need more power to generate AN signals for degrading the quality of the Alice-to-Eve link.

5 Conclusion

In this paper, we investigated a secure wireless system with a FD UAV user. To improve the SR performance, a low-complexity AIA was proposed to design two PA factors. First, in order to simplify the complicated joint optimization problem, MRT, NSP and Max-ANLNR criterions were adopted to construct the beamforming vector $\boldsymbol{v}_b$, the AN projection matrices $\boldsymbol{P}_{\rm AN}$ and $\boldsymbol{q}_{\rm AN}$. Then, it is converted to a bivariate PA optimization problem with respect to the remaining two PA factors. Actually, the simplified objective function was continuous and differentiable with respect to either the PA factor β_1 or β_2. By discussing the set of critical points, we attained the optimal value of one PA factor when the other was fixed. Finally, the AIA between β_1 and β_2 was proposed to further enhance the SR. Simulations show that the PA strategy in FD mode can improve the SR performance compared with the fixed PA factors in FD mode. And it also outperformed the case where the UAV user operated in HD mode. Moreover, the SR performance of the proposed strategy grows with increasing the value of the P_a and the number of transmit antennas.

Acknowledgements This work was supported in part by National Natural Science Foundation of China (Grant Nos. 61771244, 61501238, 61702258, 61472190, 61801453, 61271230), in part by Open Research Fund of National Key Laboratory of Electromagnetic Environment, China Research Institute of Radiowave Propagation (Grant No. 201500013), in part by Jiangsu Provincial Science Foundation (Grant No. BK20150786), in part by Specially Appointed Professor Program in Jiangsu Province, 2015, in part by Fundamental Research Funds for the Central Universities (Grant No. 30916011205), and in part by Open Research Fund of National Mobile Communications Research Laboratory, Southeast University, China (Grant Nos. 2017D04, 2013D02).

References

1 Zeng Y, Zhang R, Lim T J. Wireless communications with unmanned aerial vehicles: opportunities and challenges. IEEE Commun Mag, 2016, 54: 36–42
2 Wu Q Q, Zeng Y, Zhang R. Joint trajectory and communication design for multi-UAV enabled wireless networks. IEEE Trans Wirel Commun, 2018, 17: 2109–2121
3 Li A, Zhang W. Mobile jammer-aided secure UAV communications via trajectory design and power control. China Commun, 2018, 15: 141–151
4 Zhang G C, Wu Q Q, Cui M, et al. Securing UAV communications via trajectory optimization. In: Proceedings of IEEE Global Communications Conference, 2017
5 Chen Y, Zhao N, Ding Z, et al. Multiple UAVs as relays: multi-hop single link versus multiple dual-hop links. IEEE Trans Wirel Commun, 2018, 17: 6348–6359
6 Yang D C, Wu Q Q, Zeng Y, et al. Energy trade-off in ground-to-UAV communication via trajectory design. IEEE Trans Veh Technol, 2018, 67: 6721–6726
7 Xu Y F, Ren G C, Chen J, et al. A one-leader multi-follower bayesian-stackelberg game for anti-jamming transmission in UAV communication networks. IEEE Access, 2018, 6: 21697–21709
8 Cheng F, Zhang S, Li Z, et al. UAV trajectory optimization for data offloading at the edge of multiple cells. IEEE Trans Veh Technol, 2018, 67: 6732–6736
9 Zhang G, Yan H, Zeng Y, et al. Trajectory optimization and power allocation for multi-hop UAV relaying communications. IEEE Access, 2018, 6: 48566–48576
10 Zhou X B, Yan S H, Hu J S, et al. Joint optimization of a UAV's trajectory and transmit power for covert communications. 2018. ArXiv: 1812.00583
11 Zhong C, Yao J, Xu J. Secure UAV communication with cooperative jamming and trajectory control. IEEE Commun Lett, 2019, 23: 286–289
12 Zhou X B, Wu Q Q, Yan S H, et al. UAV-enabled secure communications: joint trajectory and transmit power optimization. IEEE Trans Veh Technol, 2019, 68: 4069–4073
13 Cai Y, Cui F, Shi Q, et al. Dual-UAV-enabled secure communications: joint trajectory design and user scheduling. IEEE J Sel Areas Commun, 2018, 36: 1972–1985
14 Liu C, Quek T Q S, Lee J. Secure UAV communication in the presence of active eavesdropper (invited paper). In: Proceedings of International Conference on Wireless Communications and Signal Processing, 2017
15 Babakhani A, Rutledge D B, Hajimiri A. Transmitter architectures based on near-field direct antenna modulation. IEEE J Solid-State Circ, 2008, 43: 2674–2692
16 Chen X M, Chen X F, Liu T. A unified performance optimization for secrecy wireless information and power transfer over interference channels. IEEE Access, 2017, 5: 12726–12736
17 Zou Y, Champagne B, Zhu W P, et al. Relay-selection improves the security-reliability trade-off in cognitive radio systems. IEEE Trans Commun, 2015, 63: 215–228
18 Lee H, Eom S, Park J, et al. UAV-aided secure communications with cooperative jamming. IEEE Trans Veh Technol, 2018, 67: 9385–9392
19 Khuwaja A A, Chen Y, Zhao N, et al. A survey of channel modeling for UAV communications. IEEE Commun Surv Tut, 2018, 20: 2804–2821
20 Negi R, Goel S. Secret communication using artificial noise. In: Proceedings of IEEE Vehicular Technology Conference, 2005. 3: 1906–1910
21 Wu Y P, Wang J B, Wang J, et al. Secure transmission with large numbers of antennas and finite alphabet inputs. IEEE Trans Commun, 2017, 65: 3614–3628
22 Ding Y, Fusco V F. A vector approach for the analysis and synthesis of directional modulation transmitters. IEEE

Trans Antenn Propagat, 2014, 62: 361–370
23 Shu F, Xu L, Wang J, et al. Artificial-noise-aided secure multicast precoding for directional modulation systems. IEEE Trans Veh Technol, 2018, 67: 6658–6662
24 Wan S M, Shu F, Lu J H, et al. Power allocation strategy of maximizing secrecy rate for secure directional modulation networks. IEEE Access, 2018, 6: 38794–38801
25 Shu F, Qin Y L, Liu T T, et al. Low-complexity and high-resolution DOA estimation for hybrid analog and digital massive MIMO receive array. IEEE Trans Commun, 2018, 66: 2487–2501
26 Shu F, Zhu W, Zhou X B, et al. Robust secure transmission of using main-lobe-integration-based leakage beamforming in directional modulation MU-MIMO systems. IEEE Syst J, 2018, 12: 3775–3785
27 Shu F, Wu X M, Hu J S, et al. Secure and precise wireless transmission for random-subcarrier-selection-based directional modulation transmit antenna array. IEEE J Sel Areas Commun, 2018, 36: 890–904
28 El Shafie A, Niyato D, Al-Dhahir N. Artificial-noise-aided secure MIMO full-duplex relay channels with fixed-power transmissions. IEEE Commun Lett, 2016, 20: 1591–1594
29 Lee J H. Full-duplex relay for enhancing physical layer security in multi-hop relaying systems. IEEE Commun Lett, 2015, 19: 525–528
30 Chen G J, Gong Y, Xiao P, et al. Physical layer network security in the full-duplex relay system. IEEE Trans Inform Forensic Secur, 2015, 10: 574–583
31 Li Y Z, Tao C, Liu L, et al. Energy-efficiency-aware relay selection in distributed full duplex relay network with massive MIMO. Sci China Inf Sci, 2017, 60: 022309
32 Li S, Li Q, Shao S H. Robust secrecy beamforming for full-duplex two-way relay networks under imperfect channel state information. Sci China Inf Sci, 2018, 61: 022307
33 Shu F, Wang M M, Wang Y X, et al. An efficient power allocation scheme for leakage-based precoding in multi-cell multiuser MIMO downlink. IEEE Commun Lett, 2011, 15: 1053–1055